Asymmetric micro-supercapacitors based on electrodeposited Ruo2 and sputtered VN films

Bouchra Asbani, Kevin Robert, Pascal Roussel, Thierry Brousse, Christophe Lethien

Asymmetric micro-supercapacitors based on electrodeposited RuO_2 and sputtered VN films

Bouchra Asbani[1,2], Kevin Robert[1,2], Pascal Roussel[3], Thierry Brousse[2,4*] and Christophe Lethien[1,2*]

[1]Institut d'Electronique, de Microélectronique et de Nanotechnologies, Université de Lille, CNRS, Centrale Lille, Université Polytechnique Hauts-de-France, UMR 8520 - IEMN, F-59000 Lille, France

[2]Réseau sur le Stockage Electrochimique de l'Energie (RS2E), CNRS FR 3459, 33 rue Saint Leu, 80039 Amiens Cedex, France

[3]Unité de Catalyse et de Chimie du Solide (UCCS), Université de Lille, CNRS, Centrale Lille, Université d'Artois, UMR 8181 – UCCS, F-59000 Lille, France

[4]Institut des Matériaux Jean Rouxel (IMN), CNRS UMR 6502 – Université de Nantes, 2 rue de la Houssinière BP32229, 44322 Nantes cedex 3, France

*Correspondence to: **Christophe.lethien@univ-lille.fr & Thierry.brousse@univ-nantes.fr**

Abstract

Research on micro-supercapacitors remains one of the most important activities in the area of electrochemical energy storage for powering smart and miniaturized electronic devices. Here we design an asymmetric micro-supercapacitor (A-MSC) combining sputtered vanadium nitride film (VN) and electrodeposited hydrous ruthenium oxide ($hRuO_2$) film. Taking advantage of their complementary electrochemical potential windows in 1M KOH electrolyte, the A-MSC achieves a cell voltage up to 1.15 V, associated to high specific

capacitance values for the device (≈ 100 mF cm^{-2}). The energy density of this asymmetric VN / $hRuO_2$ micro-supercapacitor reaches 20 µWh cm^{-2} at a power density of 3 mW cm^{-2}. Taking benefit from the asymmetric configuration, a 5-fold enhancement factor in energy density is demonstrated for the VN / $hRuO_2$ asymmetric micro-supercapacitor as compared to symmetric VN / VN and $hRuO_2$ / $hRuO_2$ microdevices.

Keywords: asymmetric micro-supercapacitors, electrodeposition, hydrous ruthenium oxide, vanadium nitride, thin films, sputtering

Introduction

Electrochemical micro-supercapacitors (MSCs) are recognized as one of the most competitive on-chip power sources for powering, among others, smart and connected devices as well as the future miniaturized Internet of Things technologies[1]. Micro-supercapacitors are a particularly intriguing novel class of miniaturized electrochemical power sources characterized by a small size, controllable patterning, high power density, long cycle life, and large scale on-chip integration capability[2–6]. However, one of the main issue to address for next generation MSCs is to increase the energy density without sacrificing the corresponding power density[7]. On the one hand, nanoporous carbon based MSCs[4,8] are an interesting solution with large cell voltage (~ 3 V) but the surface capacitance of those MSCs is limited by the charge storage mechanism within the porous electrodes based on adsorption / desorption processes. On the other hand, MSCs based on pseudocapacitive electrodes are widely investigated[6,7,9–11] mainly due to higher capacitance values but they suffer from lower cell voltage (ΔV ~ 0.6 - 0.8 V). These MSCs are composed of two symmetric electrodes meaning that the same material is used on half of the electrochemical window stability of each electrode. In that case, the total cell voltage and thus, the energy density of the MSCs is then limited. Moving from conventional symmetric to hybrid or asymmetric MSCs configuration (A-MSCs) using two different electrode materials offer a significant advantage of widened operational voltage window, and can thereby significantly enhance the energy density without sacrificing the power performance[12,13].

The fabrication of A-MSCs designed with two pseudocapacitive electrodes exhibiting complementary potential windows and high capacitance values is a promising solution to boost the energy density thanks to the concomitant increase of cell voltage. Numerous papers focusing on the fabrication of A-MSCs with pseudocapacitive materials have already been published[5,14]. RuO_2 and VN are two widely studied pseudocapacitive materials[10,15–21] with high capacitance values as “bulk” in aqueous electrolyte (> 1200 and 1300 F g^{-1} respectively) and high electronic conductivities (>10^2 S cm^{-1}) promoting fast

electron transfer. However, the gravimetric capacitance values must be carefully examined at the light of mass loading (in mg cm^{-2}) in the electrodes[22,23]. Owing to its high specific capacitance value, hydrous RuO_2 was first demonstrated[16] as a pseudocapacitive material in acidic electrolyte in 1971. Meanwhile, it was highlighted as an interesting material for electrochemical capacitors. Since RuO_2 and VN pseudocapacitive materials can be deposited as thin or thick films on functional substrates, they attracted attention towards the fabrication of miniaturized asymmetric MSCs[1].

VN has already been investigated as a negative electrode in symmetric, asymmetric or hybrid microdevices[10,20,24] due to its large specific capacitance value, high electrical conductivity and wide operation windows. Eustache[24] *et al* have reported the combined use of sputtered VN thin film with electrodeposited nickel oxide film acting as the positive electrode in 1M KOH electrolyte. This hybrid microdevice exhibits a large cell voltage, up to 1.8 V in 1M KOH, a long term cycling ability (10 000 charge / discharge cycles) with interesting energy (1.0 μWh cm^{-2}) and power (40 mW cm^{-2}) densities. Recently, the electrical and electrochemical properties of sputtered vanadium nitride thin films were investigated by our group[10,20]. In-depth investigations unveiled the charge storage process occurring within sputtered VN films in KOH electrolyte[20]. Symmetric VN / VN MSCs were developed and tested in aqueous electrolyte (1M KOH), delivering up to 20 μWh cm^{-2} energy density while keeping high power density (1 mW cm^{-2}) due to large surface capacitance value (1.2 F cm^{-2}) but low cell voltage (0.6 V)[20]. To reach this energy density value, a 16 μm-thick VN film was proposed as the pseudocapacitive electrode.

To the best of the authors' knowledge, there is a limited number of studies focusing on the design of asymmetric (micro-)supercapacitors with RuO_2 material[14,25]. Here we propose to design an asymmetric micro-supercapacitor using thin films deposition methods operating in aqueous electrolyte (0.5M H_2SO_4 and 1M KOH). The two electrodes consist in a positive hRuO_2 electrode together with a negative sputtered VN film. We propose to take advantage

of their complementary electrochemical potential windows as well as their high specific capacitance values to reach high energy density.

Vanadium Nitride (VN) and hydrous Ruthenium Oxide (RuO_2) are well known pseudocapacitive materials but their combining within an asymmetric micro-supercapacitor (MSC) was never proposed. The selected deposition methods (low temperature process) are compatible with thin film technologies allowing easy scaling-up of the fabrication process of miniaturized electrochemical capacitors with good resolution and small size. This technological transfer would not be possible if bulk synthesis methods were used to fabricate the electrodes.

Symmetric MSCs based on VN or RuO_2 electrodes, i.e. VN / VN or RuO_2 / RuO_2 MSCs, exhibit a cell voltage in the range of 0.6-0.9 V if the capacitance retention parameter is taking into account. This value is useless for powering the next generation of miniaturized electronics devices. Symmetric MSCs with higher cell voltage based on this pseudocapacitive material could be fabricated but with a significant drop of the capacitance retention. Our VN / RuO_2 A-MSC design achieves a 1.15V cell voltage.

The challenge proposed in the field of this paper consists in matching the use of VN and RuO_2 electrodes with the suitable electrolyte, considering not only the surface capacitance values but also the capacitance retention parameter. On one hand, RuO_2 is a well-known electrode material used in acidic aqueous electrolyte. On the other hand, VN exhibits a high capacitance value in alkaline aqueous solution. In the proposed study, the VN / RuO_2 A-MSC configuration is evaluated both in KOH and H_2SO_4 electrolyte. One major difficulty lies to balance the charge between the two electrodes by playing with the thickness of active materials and the suitable working potential of the electrode materials. We succeeded quite well in solving this issue since our VN / RuO2 A-MSC exhibits an energy density of 20 µWh cm^{-2} at a power density of 3 mW cm^{-2}. A comparison between symmetric (VN / VN and $hRuO_2$ / $hRuO_2$) and asymmetric MSC clearly shows a 5-fold enhancement of the energy

density. This original and promising design opens the way to potentially interesting $hRuO_2$ / VN based asymmetric microdevices.

Experimental Section

Preparation of the Si / Si_3N_4 / Pt substrate: Prior to the electrodeposition of $hRuO_2$, a platinum current collector (50 nm-thick) is deposited by atomic layer deposition method (ALD) from a TFS200 Beneq ALD reactor on a Si_3N_4 layer (300 nm-thick). The Si_3N_4 layer acts as a protective layer in order to prevent the etching of the silicon wafer by KOH electrolyte during the electrochemical experiments. This later is deposited by low-pressure chemical vapor deposition technique (LP CVD) at 800 °C (flow rates: 60 sccm for NH_3 and 20 sccm for SiH_2Cl_2) on the top of a silicon wafer (deposition pressure = 100 mTorr) using a Tempress furnace.

Sputtering deposition of VN films: VN layers are deposited on Si / Si_3N_4 substrate by magnetron sputtering deposition method using a pure metallic vanadium target (99.9%) in an Ar / N_2 atmosphere. An Alliance Concept DP650 reactor is used to deposit the VN layers. The detailed experiment set up for elaboration of VN film was previously reported in Refs[10,20].

Electrodeposition of $hRuO_2$ films: The electrodeposition of hydrous RuO_2 is performed on Si / Si_3N_4 / Pt substrate using cyclic voltammetry technique between -0.3 and 0.9 V versus Ag/AgCl at 50 mV s^{-1} from a solution based on $RuCl_3.xH_2O$ in 10^{-1} M KCl / 10^{-2}M HCl. Both deposition temperature and number of CV cycles are finely tuned to optimize the film morphology, structure and thickness.

Morphological and structural analyses: The morphological properties of the $hRuO_2$ electrode are determined using a Zeiss Ultra 55 scanning electron microscope (SEM). A 9 kW rotated anode Rigaku Smartlab diffractometer in Bragg-Brentano geometry, delivering Cu Kα radiation (λ=1.5418 Å) and a Raman spectrometer with a 471 nm UV laser source are used to study the film structure.

Electrochemical characterizations: VN and $hRuO_2$ samples (2 cm × 1 cm) were assembled in an electrochemical cell in face-to-face configuration without any separator. A well-defined surface of the VN and $hRuO_2$ thin films were in contact with the aqueous electrolytes (0.5M H_2SO_4 and 1M KOH). O-rings were used to seal the electrochemical cell and to limit the surface of the tested layers. The surface capacitance (also called areal capacitance) measured by cyclic voltammetry or galvanostatic charge / discharge cycling techniques was calculated by normalizing the capacitance (in mF) by the tested area (footprint area in cm^2), thus enabling to provide a real capacitance values in $mF.cm^{-2}$. The specific capacitance (C, $mF.cm^{-2}$), energy density (E, $\mu Wh.cm^{-2}$), and power density (P, $mW.cm^{-2}$) were calculated according to the following equations:

$$C = \frac{\int I dt}{S \Delta V} \quad \text{Eq. 1}$$

$$E = \frac{C(\Delta V)^2}{2\text{x}3.6} \quad \text{Eq. 2}$$

$$P = \frac{E}{\Delta t} \quad \text{Eq. 3}$$

where I is the current (mA), Δt is the discharge time (second), S represents the footprint area (0.405 cm^2) and ΔV is the cell voltage (V).

The electrochemical properties of $hRuO_2$ and VN electrodes are measured in a three-electrode configuration, in two aqueous electrolytes, namely KOH and H_2SO_4. The thin films act as the working electrode (WE), a platinum wire as the counter electrode, while the reference electrode is Hg/HgO for testing in KOH solution and Ag/AgCl for the electrochemical study in 0.5M H_2SO_4. Cyclic voltammetry (CV), galvanostatic charge and

discharge plots and electrochemical impedance spectroscopy (EIS) are carried out on a Biologic VMP3 potentiostat / galvanostat equipment. For the EIS experiments, the measurements are performed at open circuit voltage between 500 kHz to 10 mHz frequency range taking into account a 50 mV_{rms} sine-wave voltage amplitude.

Results and Discussion

Figure 1 describes the sketch-up of an asymmetric micro-supercapacitor (A-MSC) based on VN / $hRuO_2$ electrodes in a parallel plates configuration[1]. Sputtered vanadium nitride is used as the negative electrode while the $hRuO_2$ (positive electrode) is electrodeposited from a solution based on $RuCl_3.xH_2O$ in 10^{-1} M KCl / 10^{-2}M HCl. Both electrodes exhibit a pseudocapacitive behavior in H_2SO_4 and KOH electrolytes[9,16,20,26,27]. Knowing the electrochemical properties of both electrodes, if the charge balance is respected within the two electrodes ($Q_{RuO2} = Q_{VN}$), the cell voltage of the proposed A-MSC can be extended up to 1.15 V in 1M KOH and up to 1.35 V in 0.5M H_2SO_4. To reach this goal with our thin film technology (electrodeposition and sputtering deposition methods), it is important to have a good overview of the films properties in the two selected electrolytes and to finely adjust the thickness of the electrodes, to *in fine* balancing charges. Hence, in the first part of this paper, we investigate independently the properties of $hRuO_2$ and VN electrodes in H_2SO_4 aqueous electrolyte (**figure 2**), before the study of the assembly which is the subject of the following part.

The electrodeposition process of the $hRuO_2$ layer is firstly studied on Si / Si_3N_4 / Pt substrate. Temperature of the electrolytic solution is known to be an important parameter modifying the growth rate of the electrodeposited $hRuO_2$ film. Consequently, we started first to investigate the influence of the temperature on the film properties, in a first step at a constant number of electrodeposited cycles (200 in the present case). **The figure S1a** illustrates the scanning electron microscope (SEM) image of the $hRuO_2$ electrodeposited on Si / Si_3N_4 / Pt substrate at different temperatures. The cross-section SEM images show that the $hRuO_2$ film consists in a dense layer covered by agglomeration of particles forming a porous structure. The surface morphology of the deposited $hRuO_2$ films is very rough at 20, 30 and 40 °C, while the electrode prepared at 50 °C shows a thicker and smooth morphology. **Figure S2b** illustrates the linear dependence of the thickness with the deposition temperature of $hRuO_2$ film, always keeping constant the number of electrodeposition cycles at 200. Noteworthy, when the

electrodeposition process is achieved at 60 °C, the $hRuO_2$ film does not adhere to the substrate. Based on these optimized parameters, the deposition temperature is afterward fixed at 50 °C for the following experiments.

The figure 2a shows the SEM cross section analysis of $hRuO_2$ film deposited at 50 °C taking into account an increasing number of deposition cycles, from 100 to 600. The hydrous $hRuO_2$ film exhibits a compact morphology with a rough surface. The thickness of the $hRuO_2$ film increases with the number of electrodeposition cycles (**figure 2b**) up to ~ 700 nm for 600 electrodeposition cycles. Additionally, we observe a progressive increase of the current with the number of electrodeposition cycles as depicted in the CV plot (**figure 2b - inset**) confirming the increasing of the amount of active material. X-ray diffraction measurements in Bragg-Brentano geometry are reported for different thicknesses in **figure S1c**. After a first scan at high resolution (double 220 Ge monochromator) to check that no epitaxy between the film and the substrate occured, we decide to use a softer but with more flux Bragg-Brentano configuration. However, to avoid any saturation of the detector by the extremely intense peak of the single crystal silicon substrate, we choose to misalign it by 2°, a sufficient value to significantly decrease the non-useful huge peak-intensity of the silicon wafer, but allowing to see the other peaks issued from the active materials. Even with this high flux configuration, except peaks due to Pt current collector, no diffraction peaks corresponding to crystalline anhydrous RuO_2 are observed whatever the thickness, indicating that the as-deposited films are amorphous. The weak peak observed at $2\theta = 28.33°$ is assigned to the silicon wafer (111). To capitalize structural information on the electrodeposited $hRuO_2$ films, a complementary Raman spectroscopy study was carried out since it is also sensitive to amorphous compounds. Raman spectra were acquired on the different thicknesses RuO_2 films at room temperature (see **figure S1d**). Whatever the thickness, three broad bands located at about 509, 619, and 681 cm^{-1} are systematically observed and can be attributed [28] to namely E_g, A_{1g} and B_{2g} modes of the hydrous RuO_2.

Then, the electrochemical performance of the $hRuO_2$ thin films with various thicknesses are evaluated in 0.5M H_2SO_4 electrolyte between 0 and 1 V vs Ag/AgCl. Even if this pseudocapacitive material was already widely investigated in previous works [9,15–17,26,29–31], the electrochemical properties of our present samples have to be fully characterized in order to carefully design the A-MSC. The CV plots of 4 samples with different thicknesses are reported in **figure 2c** at 2 $mV.s^{-1}$. The CV shape is similar to that of classical pseudocapacitive RuO_2 material[13,32] where the pseudocapacitance arises from the overlap of several fast reversible redox processes occurring on the selected potential range at the surface or near-surface volume of the $hRuO_2$ films. In that case, the change of redox state of ruthenium is balanced by the surface insertion / disinsertion of protons from the H_2SO_4 aqueous electrolyte.

From the CV plots, we extract the evolution of the areal capacitance *vs* the sweep rate and the $hRuO_2$ thickness (**figure 2d**). Not surprisingly, the surface capacitance increases from 120 up to 220 $mF.cm^{-2}$ when the thickness is increased from 300 nm (100 cycles) to 700 nm (600 cycles) thus indicating that more surface is available for the 700 nm film despite a higher thickness compared to the 300 nm film. These areal capacitances challenges the best values reported so far for planar electrodes of micro-supercapacitor [17,33–36].Taking into account the potential windows used during the CV measurements (1 V), the corresponding areal capacities vary from 120 up to 220 $mC.cm^{-2}$. As already mentioned, to design an efficient asymmetric MSC with larger cell voltage than the symmetric one, it is crucial to balance the charge between the two electrodes. For that purpose, the electrochemical performance of our sputtered VN electrodes has to be carefully evaluated in 0.5M H_2SO_4 electrolyte (see **figures 2 and S2)**. Considering the electrodeposited $hRuO_2$ film as a positive electrode (fast reversible redox reactions between 0 and 1 V vs Ag/AgCl), we have to evaluate the electrochemical performance of sputtered vanadium nitride films as a negative electrode in the same conditions, *i.e* with a 0.5M H_2SO_4 aqueous electrolyte. In 2012, Pande *et al*[27] reported the cyclic voltammograms of nanostructured VN particles in 0.5M H_2SO_4: a

symmetrical rectangular-shape CV curve is observed between -0.2 and 0.6 V vs SHE. Unfortunately, no cycling performance was demonstrated in the ref[27]. In the frame of this paper, we measure the electrochemical performance of the VN electrodes between 0 and various negative potential limit values (V vs Ag/AgCl) and evaluate the capacitance retention and coulombic efficiencies. This preliminary study is mandatory to select the suitable electrochemical window from the cycling stability point of view. The performance are evaluated with a 2.3 µm-thick VN film and the measurement are carried out between 0 and -0.35, -0.4 and -0.5 V vs Ag/AgCl respectively. The results are summarized in **figure S2a-b**. When the VN films are cycled on a 0.5 V electrochemical window, the capacitance retention and the coulombic efficiency are not practical from a cycling point of view (not shown). Moving from 0.5 to 0.4 V allows to maintain a good coulombic efficiency (~ 100 %) and a retention of the initial capacitance value close to 80 % during ~ 8000 cycles (**figures S2c-d**). Unfortunately, the capacitance retention severely decreases after 8000 cycles if the VN is cycled between 0 and -0.4 V vs Ag/AgCl in 0.5M H_2SO_4 meaning that the negative limits value has to be modified. Hence, we evaluate the VN properties in a restricted electrochemical range. In that case, the coulombic efficiency (~100 %) and capacitance retention (~ 80-90 %) stay stable up to ~ 25 000 cycles (**figures S2c-d**). Based on that suitable electrochemical windows (-0.35 up to 0 V vs Ag/AgCl), we measure the electrochemical performance of various sputtered VN films having different thicknesses (1.7, 2.3 and 7 µm). Note that the structural analysis of VN films vs the thickness is shown in **Fig. 2e.** The VN films (PDF card: 00-035-0768) are polycrystalline and seems to be strongly oriented along the [111] direction for thick VN layer up to 7 µm. Except the Bragg peak at 2θ = 69° attributed to the Silicon wafer, no additional crystallized phase was identified. The intensity of this (400) silicon peak decreases for thicker VN films due to the constant penetration depth of the X-Ray beam in the Si / Si_3N_4 / VN stacked layers.

The CV curves are shown is **figure 2f** and the rectangular shape of the CV confirms the pseudocapacitive nature of the VN films in 0.5M H_2SO_4 electrolyte. From the CV plots, we

extract the areal capacitance values of the VN films which are summarized in **figure 2g**. As expected, the surface capacitance of those VN films (~ 200 mF.cm-^{2} for 7 µm-thick VN film at 2 mV.s^{-1}) exhibits values close to that of $hRuO_2$ films (~ 220 mF.cm^{-2} for 0.7 µm-thick $hRuO_2$ film at 2 mV.s^{-1}). Nevertheless, we have to keep in mind that we need to balance the charge between the two electrodes, not the capacitances. Thus, considering a 0.35 V working potential windows, the capacity of 7 µm-thick VN film is approximately 70 mC.cm^{-2} corresponding to one third of the capacitance value of the 700 nm-thick $hRuO_2$ film. Since the charge storage has to be balanced on both electrode, the thickness of the VN has to be 3 times higher (3 x 7 µm = 21 µm) which unfortunately cannot be easily reached by sputtering deposition methods[20] without delamination issues. Another solution would be to limit the capacitance value of $hRuO_2$ electrodes. As a partial conclusion, this approach is not adapted for such microdevices prepared by sputtering and electrodeposition techniques owing to the low performance of sputtered VN films in 0.5M H_2SO_4 aqueous electrolyte. This is why the as-prepared electrodes were cycled in KOH electrolyte.

Interestingly, as sputtered VN films[10,20] exhibit also a very high capacitance value in 1M KOH, we choose another attractive solution consisting in the design of a VN / $hRuO_2$ Asymmetric-MSC operating in KOH aqueous electrolyte. Many studies on nanostructured VN particles[27,37–40] or sputtered VN films[10,19,20] have demonstrated that it is possible to test this pseudocapacitive material either between -1.2 to 0 V vs Hg/HgO or between -1 to -0.4 V vs Hg/HgO in 1M KOH. Nevertheless, from a cycling stability point of view, the electrochemical potential has to be restricted to a potential window between -1 and -0.4 V vs Hg/HgO in order to maximize the capacitance retention of the VN material. The electrochemical properties of electrodeposited $hRuO_2$ films were rarely studied in KOH electrolyte[26]. We thus decide to evaluate the cycling stability of $hRuO_2$ in 1M KOH electrolyte from -0.4 V *vs* Hg/HgO up to more positive potential limits values (0.15, 0.2 and 0.3 V vs Hg/HgO). The results are shown in **figure 3a-c** for a 600 nm-thick $hRuO_2$ film (400 electrodeposited cycles). Whatever the potential window used, the CV plots at 50 mV.s^{-1}

(**figure 3a**) correspond to a pseudocapacitive material behavior [12,13,41] with good efficiency (~100 %). Moreover, the electrochemical signature of the hRuO2 films is similar to what was already reported in the literature [26,42].However, when cycled from -0.4 to 0.3 V vs Hg/HgO (operating potential windows = 0.7 V), the CV clearly exhibit an irreversible anodic process (oxidation peak) decreasing the capacitance retention of the $hRuO_2$ down to 40 % after 5 000 cycles (**figure 3c**) while the coulombic efficiency (**figure 3b**) stays stable (~100 %). Reducing the upper potential limit to 0.2 V vs Hg/HgO (operating potential windows = 0.6 V) allows enhancing the capacitance retention to 80 % after 5 000 cycles (**figure 3c**). Finally, shifting from 0.2 to 0.15 V vs Hg/HgO for the upper potential limit (i.e an operating potential window of 0.55 V) enables to prevent the anodic irreversible process allowing high stability of both coulombic efficiency and capacitance retention values (~100 %) even after 24 000 cycles (**figure 3b-c**) at 50 $mV.s^{-1}$. Using this optimized window (between -0.4 V and 0.15 V vs Hg/HgO), we tested different electrodeposited $hRuO_2$ films with various thicknesses (300, 450, 600 and 700 nm) in 1M KOH. The corresponding CVs plots of the four films at 25 mV s^{-1} are shown in **figure 3d.** Again, quasi-rectangular shape CVs characteristic of a pseudocapacitive material are observed. The capacitance value is strongly enhanced for thicker $hRuO_2$ films and the maximum capacitance value corresponds to the thicker $hRuO_2$ layer. The Nyquist plots summarizing the electrochemical impedance spectroscopy analyses of the $hRuO_2$ electrodes are reported in **figure 3e**. From these plots, we observe a typical behavior of a pseudocapacitive material with a semicircle at high frequency (illustrating the charge transfer process) and a vertical line showing the capacitive behavior of the electrodes at low frequency. Not surprisingly, the equivalent series resistance (ESR) increases for thicker $hRuO_2$ layers moving from 2.2 to 4.2 $Ohm.cm^2$ when the thickness moves from 300 to 700 nm. **Figure 3f** shows the evolution of the areal capacitance versus the sweep rate from 2 to 100 mV s^{-1} for various $hRuO_2$ thicknesses in 1M KOH. Accordingly, at 2 mV s^{-1}, the areal capacitance increases from 85 to 185 mF cm^{-2} when increasing the number of cycles from 100 to 600 (i.e thicknesses from 300 to 700 nm).

In the following part of the study, a 700 nm-thick $hRuO_2$ film is proposed as the positive electrode for the VN / $hRuO_2$ asymmetric micro-supercapacitor. The surface capacitance of the $hRuO_2$ electrode is approximately 185 $mF.cm^{-2}$ at 2 $mV.s^{-1}$. Considering an operating potential windows of 0.55 V, the charge value of the $hRuO_2$ electrode is ~ 102 $mC.cm^{-2}$. Based on our last publications on VN films[10,20]], a 2.3 µm-thick sputtered VN film (negative electrode) is necessary to balance the charge stored on the $hRuO_2$ positive electrode in such a parallel plate configuration. Indeed, the capacitance value of such 2.3 µm-thick VN film is ~ 190 $mF.cm^{-2}$ (operating potential windows = 0.6 V)[20] thus leading to a charge of 114 $mC.cm^{-2}$. The electrochemical characterizations of asymmetric VN / $hRuO_2$ (cell voltage = 1.15 V) A-MSC are compared in **figure 4** to symmetric $hRuO_2$ / $hRuO_2$ (cell voltage = 0.55 V) and VN / VN (cell voltage = 0.6 V) MSCs. The Nyquist plots of the 3 devices are reported in **figure 4a**: we observe a vertical line at low frequency and a similar capacitive behavior for both symmetric and asymmetric MSCs whatever the electrodes. Regarding the complementary operating potential windows for VN and $hRuO_2$ electrodes, we achieve galvanostatic charge/discharge (GCD) cycling in 1M KOH electrolyte, from -1 V to -0.4 V and -0.4 to 0.15 V vs Hg/HgO for the VN and $hRuO_2$ films, respectively. In symmetric MSC, the cell voltage is restricted to 0.6 V and 0.55 V for the VN / VN and $hRuO_2$ / $hRuO_2$ devices respectively meaning that the electrodes are cycled only half the cell voltage value. The galvanostatic charge / discharge plots of the symmetric and asymmetric micro-supercapacitors are shown in **figure 4b** at 3.68 $mA.cm^{-2}$ (GCD plots at different current densities are given **figure S3)**. The charge / discharge profiles of the three micro-supercapacitors exhibit a triangular shape typically observed for microdevices based on capacitive or pseudocapacitive electrodes. Note however that, while the cell voltage of VN / VN and $hRuO_2$ / $hRuO_2$ MSCs are close to 0.6 V and 0.55 V respectively, the VN / $hRuO_2$ A-MSCs can be operated up to 1.15 V. Hence, the energy density of such asymmetric microdevices is significantly enhanced. The surface capacitance of the VN / RuO_2 MSC is ~ 108 $mF.cm^{-2}$. This value challenges the best-reported capacitance by state-of-the-art planar asymmetric MSCs [35,43]. **Figure 4c** shows the Ragone plot of the VN / VN, RuO_2 / RuO_2

symmetric MSCs and VN / RuO_2 A-MSC as compared to various state of the art micro-devices. This plot evidences the evolution of the energy density vs the power density normalized by the footprint area of the devices and calculated from the discharge curves. RuO_2 and VN materials were already used as efficient electrodes in micro-supercapacitor [10,33,35,43,44]. Direct Laser Writing method was achieved to produce symmetric RuO_2 / RuO_2 MSC on flexible substrate with good energy density (~ 3 $\mu Wh.cm^{-2}$) [33]. Additionally, VN / MnO_2 asymmetric MSC operating in SiO_2 / LiTFSI water in salt electrolyte was recently proposed [43] with interesting energy density but at a low power density. The results that we obtained previously [10,44] in our group were also included in the Ragone plot to highlight the benefit of the proposed architecture. It can be noted that the thicker electrode used in our micro-devices is VN (2.3 µm). The obtained results are significantly better than the results obtained for MSCs with graphene / carbon nanotubes [45] or carbon derived carbides electrodes [4] mainly due to the use of pseudocapacitive materials in the electrode. It is well known that the capacitance of pseudocapacitive materials is higher than that of carbon based electrodes [41] owing to the fast redox reaction occurring at the surface or sub-surface of the materials. In ref [10], we proposed the fabrication of VN / VN symmetric MSC based on interdigitated topology operating in 1M KOH (orange plot). With a cell voltage of 0.6 V, this MSC exhibited a maximum areal energy density close to ~ 3 $\mu Wh.cm^{-2}$. In parallel plate configuration [1], VN / VN MSC (black plot) based on 2.3 µm-thick film electrode and tested in 1M KOH aqueous electrolyte showed an energy density of ~ 5 $\mu Wh.cm^{-2}$ while the symmetric RuO_2 / RuO_2 MSC delivered up to 6.5 $\mu Wh.cm^{-2}$ in the same electrolyte. However, this reported areal energy densities are still too low to envision the use of related electrodes for practical application to get autonomous smart and connected sensors. One strategy consists in increasing the amount of active material, that is to say to deposit thicker electrodes [46]. In that context, we previously reported 7 µm-thick and 16 µm-thick VN / VN MSC operating in a symmetrical design in 1M KOH (cell voltage ~ 0.6 V) [44]. We showed that it was possible to improve the energy density up to ~ 20 $\mu Wh.cm^{-2}$ at low power density. Due to thicker layer, we observed kinetic limitations leading to a decrease of the energy

density at high rate inducing a limitation of the rate capability of the microdevices [44]. To solve this issue, we propose in the present study to use thinner electrodes while increasing the cell voltage. This was achieved by designing asymmetric VN / RuO_2 microdevice and the cell voltage was subsequently enhanced up to 1.15 V. In that case, we observe an increase in areal energy density to ~ 20 µWh.cm^{-2} at low power density (i.e. at ~ 0.5 mW.cm^{-2}). This value is at the same level of magnitude than our previous results [44]. Nevertheless, at high power density (i.e. at 3 mW.cm^{-2}), the energy density of the VN / RuO_2 A-MSC stays close to ~ 15 µWh.cm^{-2}. This value is two times higher than that of 16 µm-thick VN / VN MSC recently reported [44] operating in the same electrolyte but using a limited cell voltage (0.6 V).

In comparison to the symmetric MSCs, the larger cell voltage of the A-MSC (1.15 V) allows maximizing the energy and power density (~ 20 µWh cm^{-2} and ~ 3 mW cm^{-2}). At 1 mW cm^{-2}, the energy density of A-MSCs (~ 20 µWh.cm^{-2}) is 5 times higher than that of either hRuO_2 / hRuO_2 or VN / VN symmetric MSCs, thus validating our approach in the design of asymmetric micro-supercapacitors based on RuO_2 and VN electrodes.

Conclusion

In this study, we carefully investigate the electrochemical performance of electrodeposited hydrous $hRuO_2$ films and sputtered vanadium nitride (VN) films as efficient electrodes for either symmetric or asymmetric micro-supercapacitors operating in 0.5M H_2SO_4 or 1M KOH aqueous electrolytes. We firstly demonstrate that an increase of the $hRuO_2$ areal capacitance with the film thickness (i.e. with the number of electrodeposition cycles) in 0.5M H_2SO_4 allows reaching 220 $mC.cm^{-2}$ (C = 220 $mF.cm^{-2}$, ΔV = 1 V) for 700 nm-thick $hRuO_2$ film. Sputtered VN electrodes show good coulombic efficiency (~ 100 %) and capacitance retention (~ 90 %) in 0.5M H_2SO_4 during 25 000 cycles. Unfortunately, in such electrolyte, we did not find suitable electrochemical conditions for cycling sputtered VN (thickness = 7 µm, C = 200 $mF.cm^{-2}$, ΔV = 0.35 V, Q = 70 $mC.cm^{-2}$) to balance the charges between the two electrodes and to take benefit from a large cell voltage (1.35 V). In 1M KOH electrolyte, we demonstrated that $hRuO_2$ film exhibits a very stable pseudocapacitive behavior with a high capacitance retention value (~ 100 %) after 24 000 charge / discharge cycles (operation potential windows = 0.55 V). Finally, we combined hRuO2 electrodeposited film with sputtered VN one to design an asymmetric micro-supercapacitor operating in 1M KOH aqueous electrolyte. The complementary working potential windows of VN and $hRuO_2$ pseudocapacitive films in 1M KOH significantly enhance the asymmetric device performance compared to symmetric ones. On one hand, either VN / VN or $hRuO_2$ / $hRuO_2$ symmetric MSCs exhibit a cell voltage of ~ 0.6 V in 1M KOH, reaching an energy density of approximately 4 $\mu Wh.cm^{-2}$ at a power density of 1 $mW.cm^{-2}$. On the other hand, the VN / $hRuO_2$ A-MSC shows a 1.15 V cell voltage and an energy density of ~ 20 $\mu Wh\ cm^{-2}$ using a power density above> 1 $mW\ cm^{-2}$. The asymmetric configuration of this MSC allows thus multiplying by a 5-fold factor the energy density of thin films micro-supercapacitors. This study gives new perspectives for improving the cell voltage of micro-supercapacitors operated in aqueous electrolyte with pseudocapacitive materials exhibiting high capacitance values and stable cycling behavior.

Acknowledgments: This research benefitted from the financial support of the ANR within the DENSSCAPIO project (ANR-17-CE05-0015-02). The authors would also like to thank the ANR STORE-EX and the RS2E for their financial support. The RENATECH network receives our utmost gratitude. Chevreul Institute (CNRS FR 2638), Ministère de l'Enseignement Supérieur et de la Recherche, Région Hauts de France and FEDER are acknowledged for supporting and funding XRD facilities.

Conflict of interest: The authors declare no conflict of interest.

References

[1] C. Lethien, J. Le Bideau, T. Brousse, Challenges and prospects of 3D micro-supercapacitors for powering the internet of things, Energy Environ. Sci. 12 (2019) 96–115. doi:10.1039/C8EE02029A.

[2] C. Shen, X. Wang, S. Li, J. Wang, W. Zhang, F. Kang, A high-energy-density micro supercapacitor of asymmetric MnO 2-carbon configuration by using micro-fabrication technologies, J. Power Sources. 234 (2013) 302–309. doi:10.1016/j.jpowsour.2012.10.101.

[3] Q. Zhang, J. Zhang, Z. Zhou, L. Wei, Y. Yao, Flexible quasi-solid-state 2.4 V aqueous asymmetric microsupercapacitors with ultrahigh energy density, J. Mater. Chem. A. 6 (2018) 20145–20151. doi:10.1039/C8TA07727D.

[4] P. Huang, C. Lethien, S. Pinaud, K. Brousse, R. Laloo, V. Turq, M. Respaud, A. Demortiere, B. Daffos, P.L. Taberna, B. Chaudret, Y. Gogotsi, P. Simon, On-chip and freestanding elastic carbon films for micro-supercapacitors, Science (80-.). 351 (2016) 691–695. doi:10.1126/science.aad3345.

[5] M.F. El-Kady, M. Ihns, M. Li, J.Y. Hwang, M.F. Mousavi, L. Chaney, A.T. Lech, R.B. Kaner, Engineering three-dimensional hybrid supercapacitors and microsupercapacitors for high-performance integrated energy storage, Proc. Natl. Acad. Sci. 112 (2015) 4233–4238. doi:10.1073/pnas.1420398112.

[6] A. Ferris, D. Bourrier, S. Garbarino, D. Guay, D. Pech, 3D Interdigitated Microsupercapacitors with Record Areal Cell Capacitance, Small. 15 (2019) 1–8. doi:10.1002/smll.201901224.

[7] B. Gao, X. Li, K. Ding, C. Huang, Q. Li, P.K. Chu, K. Huo, Recent progress in nanostructured transition metal nitrides for advanced electrochemical energy storage, J. Mater. Chem. A. 7 (2019) 14–37. doi:10.1039/c8ta05760e.

[8] M. Beidaghi, Y. Gogotsi, Capacitive energy storage in micro-scale devices: recent advances in design and fabrication of micro-supercapacitors, Energy Environ. Sci. 7 (2014) 867. doi:10.1039/c3ee43526a.

[9] A. Ferris, S. Garbarino, D. Guay, D. Pech, 3D RuO2 Microsupercapacitors with Remarkable Areal Energy, Adv. Mater. 27 (2015) 6625–6629. doi:10.1002/adma.201503054.

[10] K. Robert, C. Douard, A. Demortière, F. Blanchard, P. Roussel, T. Brousse, C. Lethien, On Chip Interdigitated Micro-Supercapacitors Based on Sputtered Bifunctional Vanadium Nitride Thin Films with Finely Tuned Inter- and Intracolumnar Porosities, Adv. Mater. Technol. 3 (2018) 1800036. doi:10.1002/admt.201800036.

[11] E. Eustache, C. Douard, A. Demortière, V. De Andrade, M. Brachet, J. Le Bideau, T. Brousse, C. Lethien, High Areal Energy 3D-Interdigitated Micro-Supercapacitors in Aqueous and Ionic Liquid Electrolytes, Adv. Mater. Technol. 2 (2017) 1700126. doi:10.1002/admt.201700126.

[12] Y. Shao, M.F. El-Kady, J. Sun, Y. Li, Q. Zhang, M. Zhu, H. Wang, B. Dunn, R.B. Kaner, Design and Mechanisms of Asymmetric Supercapacitors, Chem. Rev. 118 (2018) 9233–9280. doi:10.1021/acs.chemrev.8b00252.

[13] P. Simon, Y. Gogotsi, Perspectives for electrochemical capacitors and related devices, Nat. Mater. 19 (2020) 1151–1163. doi:10.1038/s41563-020-0747-z.

[14] Q. Jiang, N. Kurra, M. Alhabeb, Y. Gogotsi, H.N. Alshareef, All Pseudocapacitive MXene-RuO2 Asymmetric Supercapacitors, Adv. Energy Mater. 8 (2018). doi:10.1002/aenm.201703043.

[15] G. Lodi, E. Sivieri, A. De Battisti, S. Trasatti, Ruthenium dioxide-based film electrodes - III. Effect of chemical composition and surface morphology on oxygen evolution in acid solutions, J. Appl. Electrochem. 8 (1978) 135–143. doi:10.1007/BF00617671.

[16] S. Trasatti, G. Buzzanca, Ruthenium dioxide: A new interesting electrode material. Solid state structure and electrochemical behaviour, J. Electroanal. Chem. 29 (1971) 4–8. doi:10.1016/S0022-0728(71)80111-0.

[17] J.H. Lim, D.J. Choi, H.K. Kim, W.I.I. Cho, Y.S. Yoon, Thin film supercapacitors using a sputtered RuO2 electrode, J. Electrochem. Soc. 148 (2001) A275. doi:10.1149/1.1350666.

[18] D. Choi, G.E. Blomgren, P.N. Kumta, Fast and reversible surface redox reaction in nanocrystalline vanadium nitride supercapacitors, Adv. Mater. 18 (2006) 1178–1182. doi:10.1002/adma.200502471.

[19] Y. Borjon-Piron, A. Morel, D. Bélanger, R.L. Porto, T. Brousse, Suitable Conditions for the Use of Vanadium Nitride as an Electrode for Electrochemical Capacitor, J. Electrochem. Soc. 163 (2016) A1077–A1082. doi:10.1149/2.1221606jes.

[20] K. Robert, D. Stiévenard, D. Deresmes, C. Douard, A. Iadecola, D. Troadec, P. Simon, N. Nuns, M. Marinova, M. Huvé, P. Roussel, T. Brousse, C. Lethien, Novel insights into the charge storage mechanism in pseudocapacitive vanadium nitride thick films for high-performance on-chip micro-supercapacitors, Energy Environ. Sci. 13 (2020) 949–957. doi:10.1039/c9ee03787j.

[21] I.-H. Kim, K.-B. Kim, Electrochemical Characterization of Hydrous Ruthenium Oxide Thin-Film Electrodes for Electrochemical Capacitor Applications, J. Electrochem. Soc. 153 (2006) A383. doi:10.1149/1.2147406.

[22] Y. Gogotsi, P. Simon, True Performance Metrics in Electrochemical Energy Storage, Science (80-.). 334 (2011) 917–918. doi:10.1126/science.1213003.

[23] D. Belanger, W. Sugimoto, A. Balducci, T. Brousse, J.W. Long, Perspective—A Guideline for Reporting Performance Metrics with Electrochemical Capacitors: From Electrode Materials to Full Devices, J. Electrochem. Soc. 164 (2017) A1487–A1488.

doi:10.1149/2.0851707jes.

[24] E. Eustache, R. Frappier, R.L. Porto, S. Bouhtiyya, J.F. Pierson, T. Brousse, Asymmetric electrochemical capacitor microdevice designed with vanadium nitride and nickel oxide thin film electrodes, Electrochem. Commun. 28 (2013) 104–106. doi:10.1016/j.elecom.2012.12.015.

[25] J. Zhang, J. Jiang, H. Li, X.S. Zhao, A high-performance asymmetric supercapacitor fabricated with graphene-based electrodes, Energy Environ. Sci. 4 (2011) 4009–4015. doi:10.1039/C1EE01354H.

[26] S. Ardizzone, G. Fregonara, S. Trasatti, “Inner” and “outer” active surface of RuO2 electrodes, Electrochim. Acta. 35 (1990) 263–267. doi:10.1016/0013-4686(90)85068-X.

[27] P. Pande, P.G. Rasmussen, L.T. Thompson, Charge storage on nanostructured early transition metal nitrides and carbides, J. Power Sources. 207 (2012) 212–215. doi:10.1016/j.jpowsour.2012.01.028.

[28] S.Y. Mar, C.S. Chen, Y.S. Huang, K.K. Tiong, Characterization of RuO2 thin films by Raman spectroscopy, Appl. Surf. Sci. 90 (1995) 497–504. doi:10.1016/S0040-6090(96)09545-4.

[29] S. Makino, T. Ban, W. Sugimoto, Towards Implantable Bio-Supercapacitors: Pseudocapacitance of Ruthenium Oxide Nanoparticles and Nanosheets in Acids, Buffered Solutions, and Bioelectrolytes, J. Electrochem. Soc. 162 (2015) A5001–A5006. doi:10.1149/2.0021505jes.

[30] A. Ponrouch, S. Garbarino, E. Bertin, D. Guay, Ultra high capacitance values of Pt@RuO 2 core-shell nanotubular electrodes for microsupercapacitor applications, J. Power Sources. 221 (2013) 228–231. doi:10.1016/j.jpowsour.2012.08.033.

[31] Y.S. Yoon, W.I. Cho, J.H. Lim, D.J. Choi, Solid-state thin-film supercapacitor with

ruthenium oxide and solid electrolyte thin films, J. Power Sources. 101 (2001) 126–129. doi:10.1016/S0378-7753(01)00484-0.

[32] P. Simon, Y. Gogotsi, Materials for electrochemical capacitors, Nat. Mater. 7 (2008) 845–854. doi:10.1038/nmat2297.

[33] K. Brousse, S. Pinaud, S. Nguyen, P.F. Fazzini, R. Makarem, C. Josse, Y. Thimont, B. Chaudret, P.L. Taberna, M. Respaud, P. Simon, Facile and Scalable Preparation of Ruthenium Oxide-Based Flexible Micro-Supercapacitors, Adv. Energy Mater. 10 (2020) 1–9. doi:10.1002/aenm.201903136.

[34] W. Si, C. Yan, Y. Chen, S. Oswald, L. Han, O.G. Schmidt, On chip, all solid-state and flexible micro-supercapacitors with high performance based on MnOx/Au multilayers, Energy Environ. Sci. 6 (2013) 3218–3223. doi:10.1039/c3ee41286e.

[35] T.M. Dinh, F. Mesnilgrente, V. Conédéra, N.A. Kyerematenga, D. Pech, Realization of an Asymmetric Interdigitated Electrochemical Micro-Capacitor Based on Carbon Nanotubes and Manganese Oxide, J. Electrochem. Soc. 162 (2015) 2016–2020. doi:10.1149/2.0431510jes.

[36] M.K. Hota, Q. Jiang, Z. Wang, Z.L. Wang, K.N. Salama, H.N. Alshareef, Integration of Electrochemical Microsupercapacitors with Thin Film Electronics for On-Chip Energy Storage, Adv. Mater. 31 (2019) 1–9. doi:10.1002/adma.201807450.

[37] D. Choi, G.E. Blomgren, P.N. Kumta, Fast and reversible surface redox reaction in nanocrystalline vanadium nitride supercapacitors, Adv. Mater. 18 (2006) 1178–1182. doi:10.1002/adma.200502471.

[38] P.J. Hanumantha, M.K. Datta, K. Kadakia, C. Okoli, P. Patel, P.N. Kumta, Vanadium nitride supercapacitors: Effect of Processing Parameters on electrochemical charge storage behavior, Electrochim. Acta. 207 (2016) 37–47. doi:10.1016/j.electacta.2016.04.058.

[39] B. Chen, L. Han, B. Li, Pseudo-capacitance behaviour of reactively sputtered vanadium nitride electrodes deposited at different working pressures: The critical role of surface chemistry, Mater. Chem. Phys. 236 (2019) 121820. doi:10.1016/j.matchemphys.2019.121820.

[40] A. Djire, P. Pande, A. Deb, J.B. Siegel, O.T. Ajenifujah, L. He, A.E. Sleightholme, P.G. Rasmussen, L.T. Thompson, Unveiling the pseudocapacitive charge storage mechanisms of nanostructured vanadium nitrides using in-situ analyses, Nano Energy. 60 (2019) 72–81. doi:10.1016/j.nanoen.2019.03.003.

[41] T. Brousse, D. Bélanger, J.W. Long, To Be or Not To Be Pseudocapacitive?, J. Electrochem. Soc. 162 (2015) A5185–A5189. doi:10.1149/2.0201505jes.

[42] Y.G. Wang, Z.D. Wang, Y.Y. Xia, An asymmetric supercapacitor using RuO2/TiO2 nanotube composite and activated carbon electrodes, Electrochim. Acta. 50 (2005) 5641–5646. doi:10.1016/j.electacta.2005.03.042.

[43] J. Qin, S. Wang, F. Zhou, P. Das, S. Zheng, C. Sun, X. Bao, Z.S. Wu, 2D mesoporous MnO2 nanosheets for high-energy asymmetric micro-supercapacitors in water-in-salt gel electrolyte, Energy Storage Mater. 18 (2019) 397–404. doi:10.1016/j.ensm.2018.12.022.

[44] K. Robert, D. Stievenard, D. Deresmes, D. Troadec, C. Douard, A. Iadecola, M. Huvé, M. Marinova, P. Simon, N. Nuns, P. Roussel, T. Brousse, C. Lethien, Novel insights into the charge storage mechanism in pseudocapacitive vanadium nitride thick films, Energy Environ. Sci. 13 (2020) 949–957. doi:10.1039/c9ee03787j.

[45] J. Lin, C. Zhang, Z. Yan, Y. Zhu, Z. Peng, R.H. Hauge, D. Natelson, J.M. Tour, 3-Dimensional Graphene Carbon Nanotube Carpet-Based Microsupercapacitors With High Electrochemical Performance, Nano Lett. 13 (2013) 72–78. doi:10.1021/nl3034976.

[46] S. Ouendi, K. Robert, D. Stievenard, T. Brousse, P. Roussel, C. Lethien, Sputtered tungsten nitride films as pseudocapacitive electrode for on chip micro-supercapacitors, Energy Storage Mater. 20 (2019) 243–252. doi:10.1016/j.ensm.2019.04.006.

List of the figures and captions

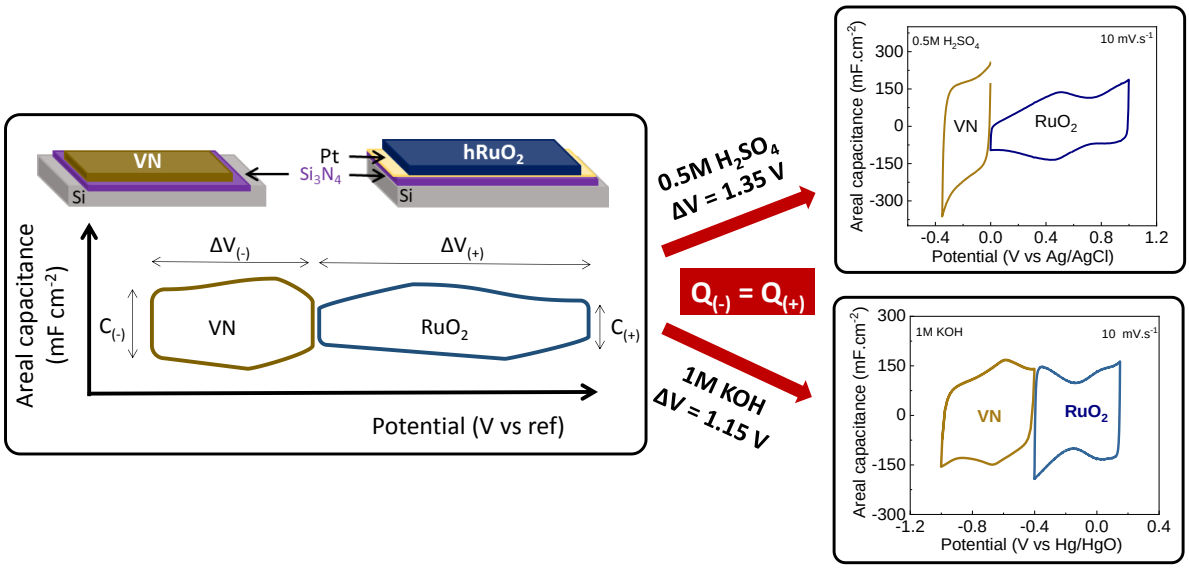

Fig. 1 | Sketch up of the VN / $hRuO_2$ asymmetric micro-supercapacitor (A-MSC) in face-to-face topology operating in 0.5M H_2SO_4 and 1M KOH aqueous electrolytes.

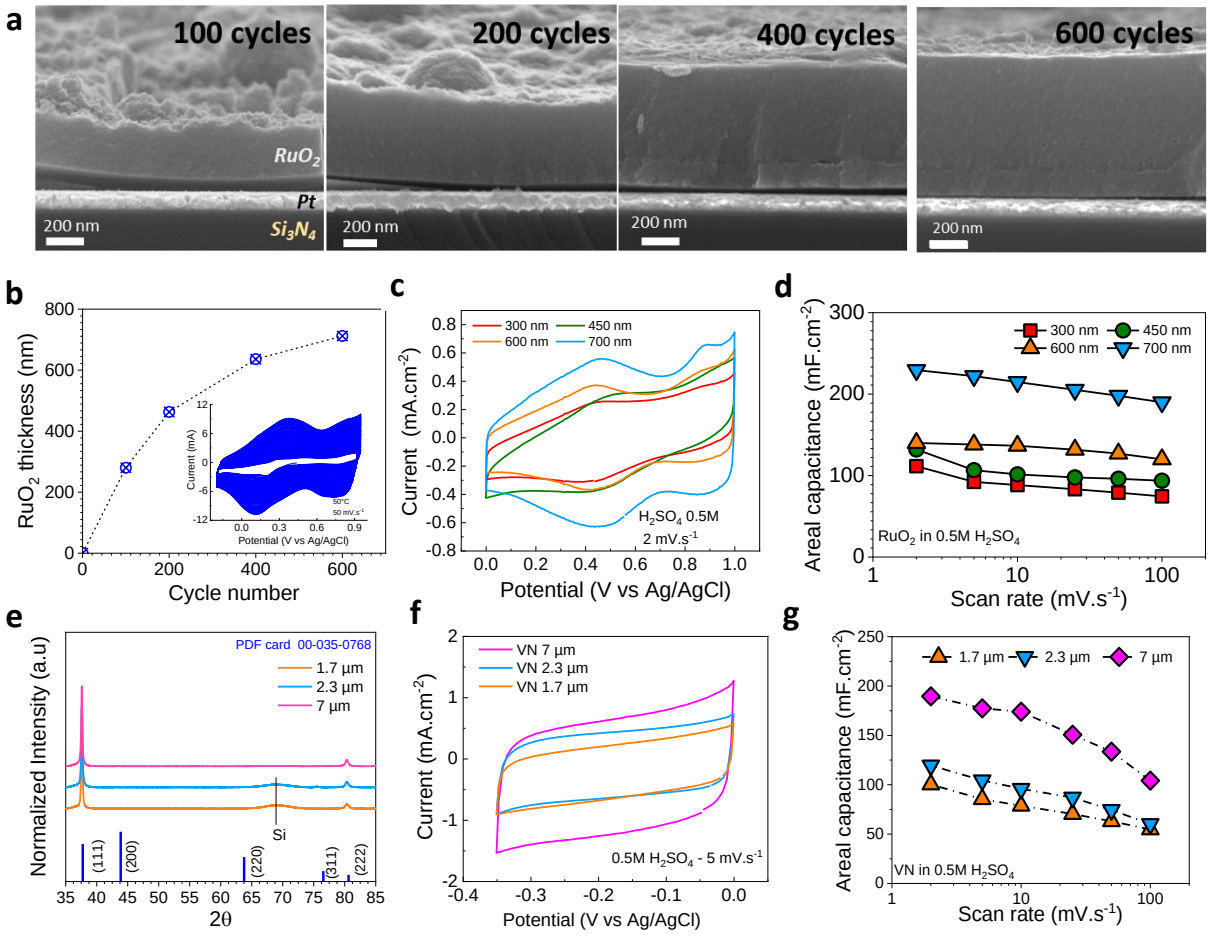

Fig. 2 | Properties of the RuO_2 and VN thin film electrodes. a. SEM cross section of $hRuO_2$ electrodeposited on Si / Si_3N_4 / Pt substrate vs the number of deposition cycles. **b.** Evolution of the $hRuO_2$ thickness *vs* the number of electrodeposition cycles. The inset shows the CV cycles carried out at 50 mV s^{-1} & 50 °C between -0.3 and 0.9 V in an electrolytic solution based on $RuCl_3$ particles dissolved in 10^{-1} M KCl / 10^{-2} M HCl. **c-d.** Electrochemical properties of the RuO_2 films in 0.5M H_2SO_4 for various film thicknesses. **e.** X-Ray Diffraction Analyses of vanadium nitride films (1.7, 2.3 and 7 µm). **f-g.** Electrochemical performance of the VN films (various thicknesses) in 0.5M H_2SO_4.

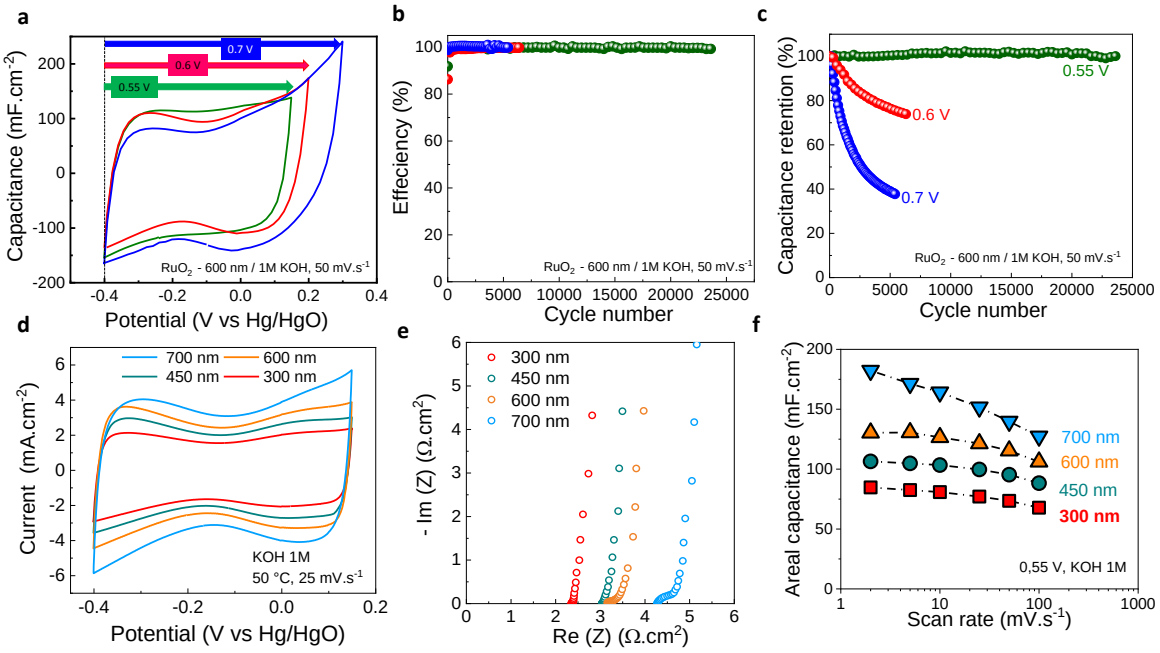

Fig. 3 | Electrochemical properties of the $hRuO_2$ films in 1M KOH. a. CV plots of the $hRuO_2$ films (400 electrodeposition cycles / 600 nm) between -0.4 and 0.15, 0.2 and 0.3 V vs Hg/HgO at 50 $mV.s^{-1}$. **b-c.** Evolution of the coulombic efficiency and the capacitance retention for $hRuO_2$ films (400 electrodeposition cycles / 600 nm) vs the cycle number at 50 $mV.s^{-1}$ and the proposed electrochemical windows. **d.** CV plots of the $hRuO_2$ films with different thickness between -0.4 and 0.15 V vs Hg/HgO at 25 $mV.s^{-1}$. **e.** Electrochemical Impedance Spectroscopy measured in 1M KOH for RuO_2 films with various thicknesses. **f.** Evolution of the areal capacitance values versus sweep rate and film thicknesses.

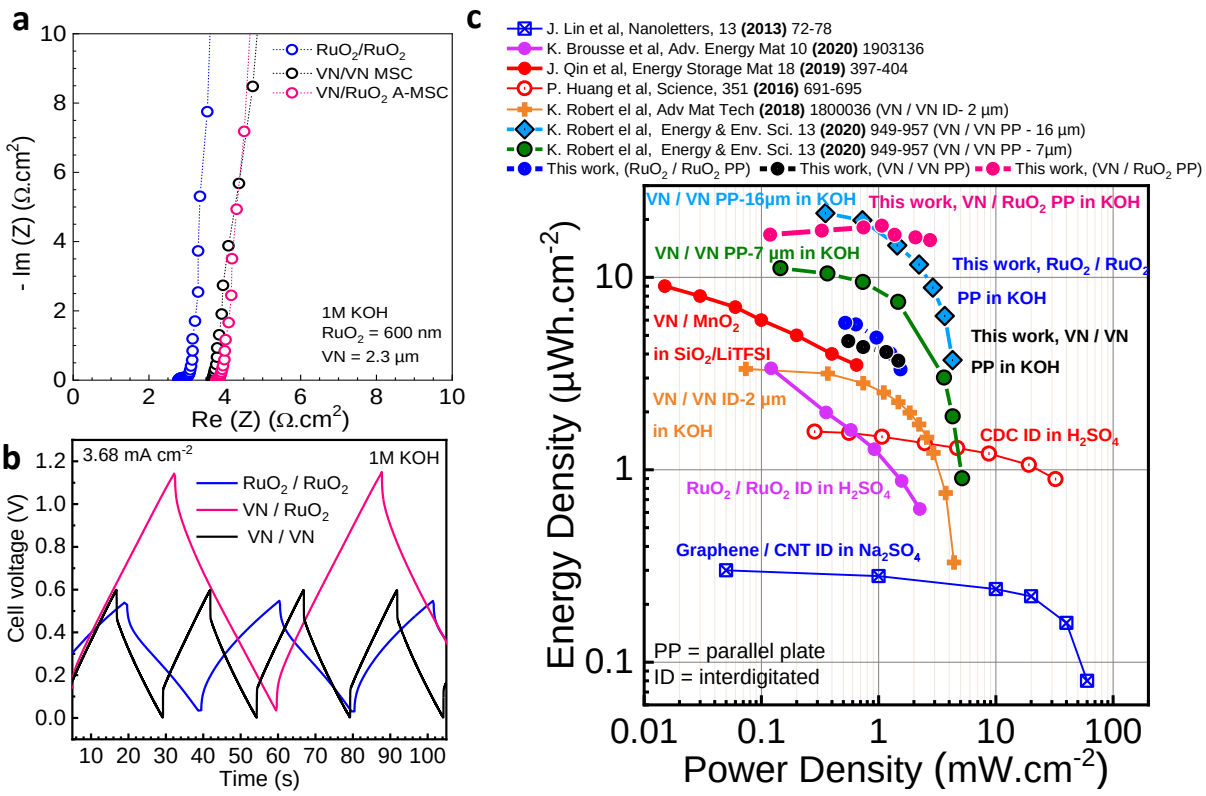

Fig. 4 | Electrochemical performance of the symmetric and asymmetric MSC tested in 1M KOH electrolyte. a. Nyquist plots of the three MSCs (symmetric $hRuO_2$ / $hRuO_2$, VN / VN MSC and VN / $hRuO_2$ asymmetric) validating the capacitive behavior of the devices in both symmetric and asymmetric configurations. **b.** Galvanostatic charge and discharge plots of the three micro-supercapacitors measured in 1M KOH at 3.68 $mA.cm^{-2}$: for the A-MSC, the thicknesses of the positive ($hRuO_2$) and negative (VN) electrodes have been tuned in order to balance the capacity of each electrode in both cases. A 2.3 µm-thick VN film and a 700 nm-thick $hRuO_2$ (600 cycles) exhibit the same areal capacitance and the same electrochemical windows (~ 0.6 V), thus storing the same charge on each electrode. **c**. Ragone plot of the $hRuO_2$ / $hRuO_2$, VN / VN and VN / $hRuO_2$ microdevices tested in 1M KOH as compared to stat of the art micro-devices [4,10,33,44,45] and demonstrating the gain measured with the asymmetric configuration.

Supporting information

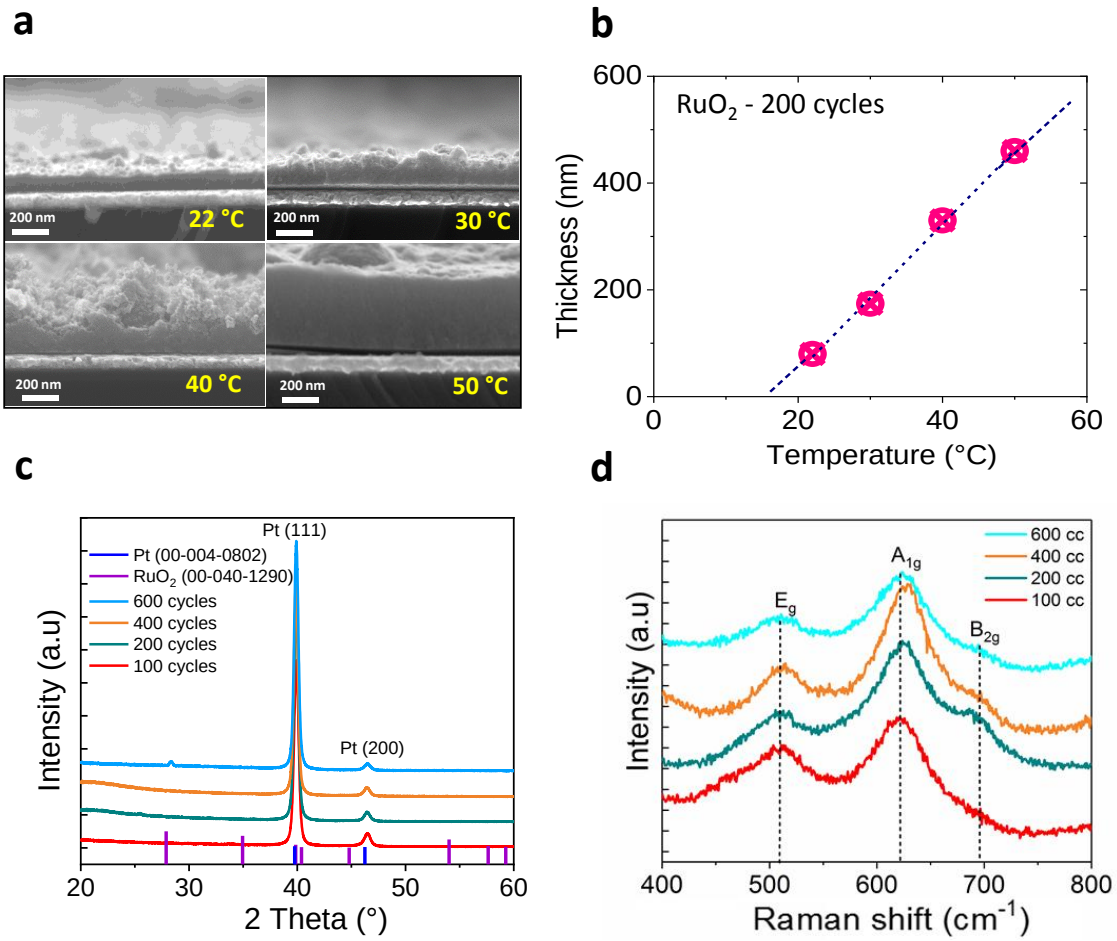

Fig. S1 | a. SEM cross-section analysis of electrodeposited hRuO2 films vs the temperature. **b.** Evolution of the film thickness vs the temperature**.** Structural analyses of various $hRuO_2$ films using **c.** X-Ray Diffraction technique and **d.** Raman spectroscopy method.

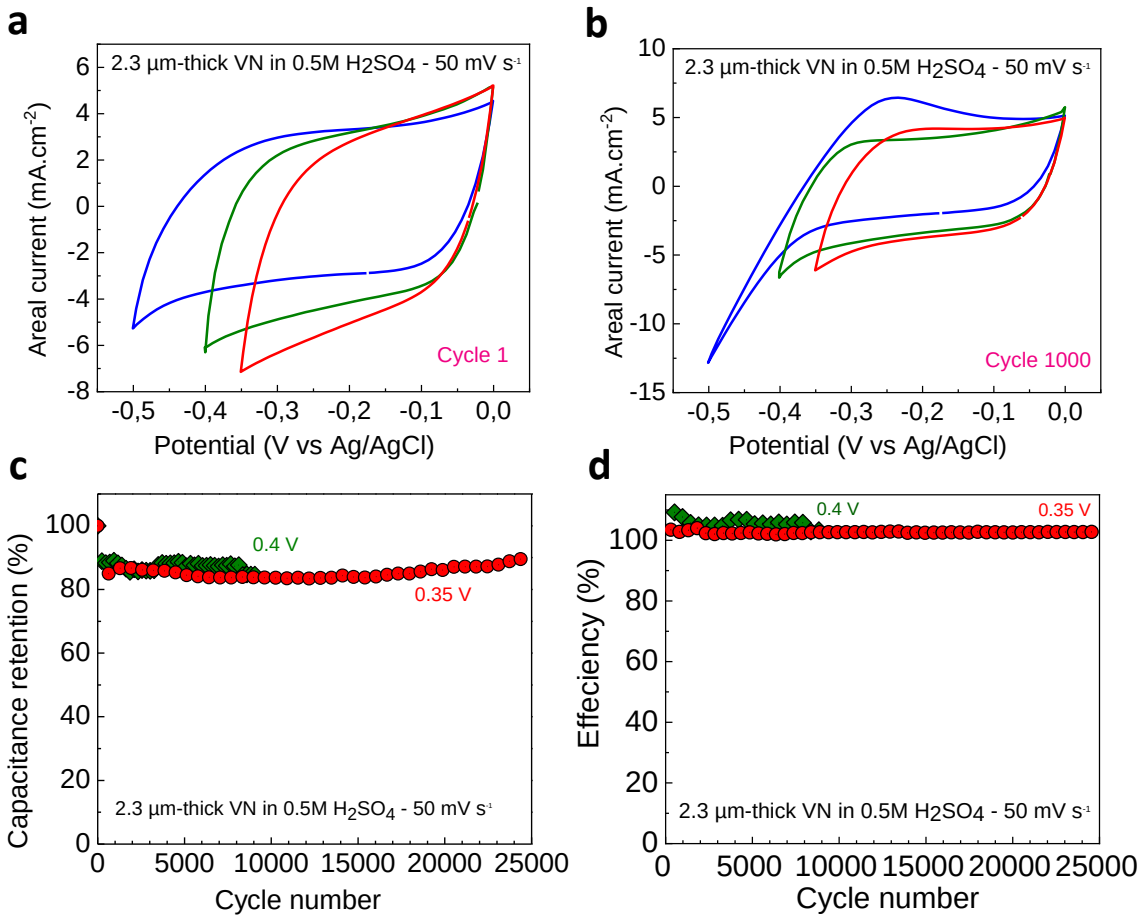

Fig. S2 | Electrochemical performance of the VN film in 0.5M H_2SO_4. a. CV plots of 2.3 µm-thick VN film tested between 0 and - 0.35 V, - 0.4 and -0.5 V vs Ag/AgCl respectively (**1st cycle**). **b.** CV plots of 2.3 µm-thick VN film tested between 0 and - 0.35 V, - 0.4 and -0.5 V vs Ag/AgCl respectively (**1000th cycle**). **c-d.** Evolution of the capacitance retention and coulombic efficiency of the VN film in 0.5 M H_2SO_4 at 50 $mV.s^{-1}$.

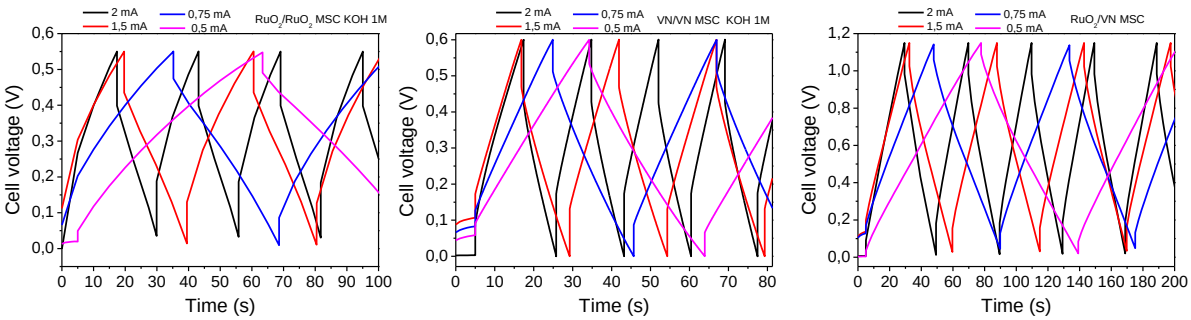

Fig. S3 | Galvanostatic Charge and Discharge plots of the VN / $hRuO_2$ A-MSC in 1M KOH at different current densities.